A high-performance, flexible, and cost-efficient auditory evoked response recording system appropriate for research purposes

Author Listing:

- [names] Joaquin T. [surname] Valderrama [a,*]
- [name] Angel [surname] de la Torre [a]
- [name] Isaac [surname] Alvarez [a]
- [names] Jose Carlos [surname] Segura [a]
- [name] Manuel [surname] Sainz [b,c]
- [names] Jose Luis [surname] Vargas [b]

Affiliations:

[*] Corresponding author. Address: C/ Periodista Daniel Saucedo Aranda s/n, 18071, Granada, Spain. Tel.: +34 958 240 840; fax: +34 958 240 831. E-mail address: jvalderrama@ugr.es; joaquint.valderrama@gmail.com (J. T. Valderrama).

[a] Department of Signal Theory, Telematics and Communications, CITIC-UGR, University of Granada, Granada, Spain.

[b] ENT Service, San Cecilio University Hospital, Granada, Spain.

[c] Department of Surgery and its Specialties, University of Granada, Granada, Spain.

Abstract:

The recording of auditory evoked responses (AER) is used in hospitals and clinics worldwide for hearing impairments detection and threshold estimation, and in research centers to understand and model the mechanisms involved in the process of hearing. This paper describes a high-performance, flexible, and inexpensive AER recording system. A full description of the hardware and software modules that compose the AER recording system is provided in this article. The performance of this system is evaluated by five experiments with both real and artificially synthesized auditory brainstem response (ABR) and middle latency response (MLR) signals at different intensity levels and stimulation rates. The results of this study point out that the flexibility of the described system is appropriate to record AER signals in several recording conditions. The AER recording system described in this article gives users a full control of the parameter settings involved in the AER recording process, incorporates a platform through which users are allowed to implement advanced signal processing methods, and its manufacturing cost is significantly lower than other current commercial alternatives. These advantages could be suitable in many research applications in the field of Audiology.

Keywords: Auditory evoked responses (AER); auditory brainstem response (ABR); middle latency response (MLR); evoked potentials; biomedical amplifier.

List of abbreviations:

AER: auditory evoked response; ABR: auditory brainstem response; MLR: middle latency response; ECochG: electrocochleography; SNR: signal-to-noise ratio; CMRR: common mode rejection ratio; EEG: electroencephalogram; AD/DA: analog to digital / digital to analog; ISI: interstimulus interval; CONV: conventional; MLS: maximum length sequences; CLAD: continuous loop averaging deconvolution; QSD: quasiperiodic sequence deconvolution; LS: least-squares; RSA: randomized stimulation and averaging; dB: decibel; I/O: input / output; nHL: normal hearing level; SPL: sound pressure level; ECochG: electrocochleography; ERP: event related potential.

Text body:

1. INTRODUCTION

The auditory evoked response (AER) is the electrical activity of the nervous system in response to a stimulus. This electrical activity is characterized by a number of voltage peaks of very low amplitude, called evoked potentials, which are generated in different parts of the auditory pathway. These evoked potentials can be classified according to their generator site and the time between the stimulus onset and the occurrence of the peaks (peak latency), which ranges between 1 ms and 0.5 second. The recording of the AER has been extensively used in human and animal studies for both clinical and research purposes due to its noninvasive nature. The auditory brainstem response (ABR) and the middle latency response (MLR) are AERs generated in the brainstem and in the auditory cortex respectively [7]. The ABR comprises a number of waves that occur during the first 10 ms from stimulus onset. These

ABR waves are identified by sequential roman numerals as originally proposed by Jewett and Williston [17]. Although up to seven peaks can be seen in the ABR, the most robust waves are I, III, and V. The MLR have latencies from 10 to 60 ms and comprise the components N_a, P_a, N_b, P_b. The longer component of the MLR is usually affected by attention and is difficult to record under sedation. The recording of these signals is commonly used in hospital and clinics worldwide as a hearing screening tool, to detect the hearing threshold, and hearing impairments such as vestibular schwannoma and Ménière’s disease. Furthermore, the analysis of the AER may help understand the underlying mechanisms of the process of hearing [20,23,34]. The recording process of these signals involves the setting-up of a wide range of factors [26].

This paper describes in detail a high-performance, flexible, and inexpensive AER recording system. Although there already exist several clinical systems that allow the recording of the AER, most of them are expensive, the control over most of the parameter settings is limited, and give no access to raw recorded data [1]. In contrast, the AER recording system described in this article gives users a full control of the parameter settings. Users are able to set the intensity level of stimulation, select the number of auditory responses for average, use the conventional method of stimulation or any other more advanced technique, set the stimulation frequency, select the analog-to-digital sampling frequency, choose the order and band-pass cut-off frequencies for digital filters, select the polarity of stimulation and nature of the stimuli (clicks, chirps, tone pips, etc.), or implement advanced artifact rejection techniques. In addition, this system gives access to raw recording data, thus advanced signal processing methods can be implemented offline. The performance of this system is evaluated through five experiments with both real and artificially synthesized ABR and MLR signals recorded at different intensity levels and stimulation rates. The flexibility, along with the high-performance and cost-efficient nature of the AER recording system described in this article, might be suitable to carry out research activities of different nature in the field of Audiology.

2. SYSTEM ARCHITECTURE

2.1. System overview

The procedure for recording the AER is schemed in figure 1. This process includes the presentation of auditory stimuli and the recording of their corresponding electrical response (sweep) by surface electrodes. A high amplification of this signal is required due to the low amplitude of the AER (usually less than 1 μV). The recorded signal is usually highly contaminated by different types of artifacts, such as myogenic noise related to the muscular activity of the subject, electrical noise derived from the amplifier, electromagnetic and radiofrequency interferences, etc. The conventional method used to reduce the effects of these artifacts and improve the signal-to-noise ratio (SNR) of the response is the average of a large number of sweeps whose corresponding stimuli are periodically presented [4,8,37]. This system is battery powered in order to reduce the artifact generated by the electric power network. The stimulation of the auditory system is conventionally performed by 0.1 ms duration clicks in rarefaction polarity in order to evoke a synchronous firing of a large number of neurons, however, this system allows the implementation of other stimulus types such as tone burst, filtered clicks, chirps, noise stimuli, and speech stimuli [13]. The intensity level can be controlled by setting the amplitude of the stimulation signal. A signal composed of a burst of stimuli is generated by the laptop for both stimulation and synchronization purposes. This signal is sent synchronously by the left and right outputs of an analog-to-digital / digital-to-analog (AD/DA) soundcard. The right output is connected to the left input for the synchronization of the stimuli. The left output is connected to a pair of insert earphones, through which the stimulation signal excites the auditory system of the subject, thus generating the AER. This biological signal, plus noise, is recorded by three electrodes placed on the skin at different positions on the head. The electroencephalogram (EEG) recorded by the electrodes is amplified and band-pass filtered. The auditory response after filtering and amplification is recorded synchronously along with the synchronization signal by the right and left inputs of the external AD/DA soundcard. The software routines of this system implement the digital signal processing methods necessary to obtain the AER. Figure 2 shows a picture of the electronics of the amplifier (left) and the hardware elements that compose the AER recording system (right). Table 1 presents a rough cost list of the elements that include the AER recording system. This table was built considering the price list of a well-known international electronics supplier. The cost analysis presented in this table shows that the cost of the elements and materials involved in the AER recording system prototype described in this paper (laptop not included) is around 950 USD.

2.2. Hardware specifications

2.2.1. Amplifier

The amplifier is composed of four stages: preamplification, band-pass filtering, amplification, and active ground circuitry. The electronic schematic of the amplifier is shown in figure 3. The stage of preamplification provides a moderate gain in order to avoid saturation in later stages. This stage is based on the instrumental amplifier INA128 (Texas Instruments Inc., Dallas, TX). This differential amplifier was chosen because of its high common mode rejection ratio (CMRR), low power, low noise ($8\,nV/\sqrt{Hz}$), and easy control of the gain. The band-pass filtering stage removes the frequencies out of the scope of the AER, amplifying only the band of interest. This stage comprises four second order Sallen-Key filters (2 x high pass & 2 x low pass). The values of the resistors and capacitances that implement the filtering stage define the bandwidth of the amplifier. The bandwidth of the amplifier must be selected considering the characteristic frequencies of each AER. Table 2 shows the characteristic bandwidth for recording ABR and MLR signals, along with suggested values of resistors and capacitances that implement the high pass and low pass filtering stages of the amplifier. These analog filters insert a phase distortion on the recorded signal that must be adjusted by software. This phase shift is 560 μs for the ABR amplifier and 80 μs for the MLR amplifier. The amplification stage after filtering sets the required level of amplitude on the EEG to be recorded by the analog to digital converter. The active ground circuit is designed to reduce the common mode voltage of the recorded signal. The electric field generated by the electric network can induce a common mode voltage on the subject. This common mode voltage is amplified, inverted, and inserted back to the subject by the active ground circuit, thus reducing significantly the common mode voltage on the subject. The operational amplifiers OPA227 (Texas Instruments Inc., Dallas, TX) used in this circuit were chosen because of their very low noise voltage ($3\,nV/\sqrt{Hz}$), high CMRR (130 dB), and high precision. The Bode diagrams on Figure 4 show the bandwidth and the phase shift of the amplifiers for ABR and MLR signals. The gain of the amplifier reaches the value G_A = 20.000 (86 dB) for the band-pass frequencies, with a filter slope of 24 dB/oct. Figure 5 represents a linearity analysis for the ABR amplifier. This figure represents a 10 ms sinusoidal signal inserted on the amplifier (input signal) versus its corresponding output signal. The slope of this curve represents the gain of the amplifier (86 dB). The amplitude of the input signal was chosen to obtain a slightly saturated output signal. The frequency of the input signal was set on 1087 Hz to obtain an output signal with phase distortion zero. This analysis suggests that the behavior of the amplifier is especially lineal when the input signal is in the range [-0.3 +0.3] mV, a common situation considering that the recorded EEG does not usually exceed 50 µV [13]. Thus, the dynamic range of the amplifier is 600 µv. The consumption of this circuit is 28.2 mA, which gives the device an operating time of more than 6 hours for standard rechargeable 9V batteries. The safety of the subject under exploration is granted, on one hand, by the battery powered nature of the system, which prevents any possible electrical shock derived from the electrical network; and on the other hand, by the 1 MΩ resistor that connects the active ground electrode to the subject, which limits the leakage current introduced to the subject to 9 µA, meeting the electrical safety requirements of the international standard IEC 60601-1 [38].

2.2.2. Electrodes

Electrodes transform ionic currents (mechanism of conduction of bioelectrical signals on tissues) into electrical currents that conduct the evoked potentials from the subject to the recording system. Since the electrodes are the first components on signal recording, the noise level generated at them should be minimized. The preferable electrodes to reduce contact potential, typically used in AER recording, are silver coated with silver chloride (Ag/AgCl) surface electrodes, composed of a silver conductor (electrode) immersed into a silver chloride salt dissolution (electrolyte). Electrolytic paste is used as a mean of union between the electrode and the skin in order to reduce the contact electrode impedance. The contact impedance of the junction between the scalp and the electrodes should be kept as low as possible to minimize the magnitude of induced electromagnetic artifacts and to reduce the capacitive coupling effects of the electrode cables and external power lines [13,26]. This contact impedance can be reduced by a softly scrape of the skin with alcohol or other cleansing agent. The electrode-skin contact impedance can be measured either by any commercial alternating-current impedance meter, or by implementing the circuit diagram of any impedance meter described in the literature, e.g., [11,12]. Impedances lower than 5 kΩ at the working frequencies can be considered acceptable. The electrodes impedance should be balanced to avoid common mode artifacts. The placement of the electrodes can be done in accordance with the standard positions defined by the International 10-20 and 10-10 Systems [16,19]. Active, ground, and reference electrodes can be situated at the high forehead (Fz), low forehead (Fpz), and ipsilateral mastoid (TP9/TP10) respectively, as shown in figure 1. Active and reference electrodes are connected to the differential inputs of the amplifier. The ground electrode connects the active ground input of the amplifier.

2.2.3. Analog-to-Digital conversion

The analog-to-digital conversion is carried out by an external soundcard connected to the laptop through the USB port. This device presents the advantages of simplicity and a better performance than most of soundcards integrated on laptops. Table 3 shows a summary of the features of the AD/DA soundcard. The number of bits of quantization and the sampling rate can be controlled by the user.

The amplitude precision of the analog-to digital conversion is determined by the number of bits of quantization. Considering the recording of ABR signals, the analog-to-digital converter should be able to measure on the range 2 nV (10% precision of a standard 20 nV amplitude of a wave II) to 200 μV (highest expected recorded level of an EEG). This is a ratio of 100.000, and corresponds to a dynamic range of 100 dB. Considering that an AD/DA of n bits has a dynamic range of 6·n dB, the required number of bits of the AD/DA to be able to record ABR with a precision of a 10% is about 16 bits. In addition to this, the process of sweeps averaging increases the precision of the measure, reducing the quantization noise [26]. Therefore, the use 16 bits of quantization is enough to record AER with sufficient precision.

The sampling rate must be greater than the double of the highest frequency component present in the signal in order to prevent aliasing [21]. However, the low-pass filters of the filtering stage in the amplifier just attenuate (not eliminate) the frequency components greater than the cutoff frequency (f_c). The aliasing errors from all frequency components would be prevented only when the sampling rate is set to twice the frequency at which the filter attenuates the signal by more than the dynamic range of the AD/DA. Considering a standard AD/DA converter, the frequency at which this occur is $f' = f_c \cdot 2^{(D-3)/S}$, where f_c is the cutoff frequency, D is the dynamic range of the AD/DA in dB, and S is the slope in dB per octave [26]. Therefore, to avoid even 1-bit aliasing errors, the sampling rate (f_s) must be $f_s = 2 \cdot f_c \cdot 2^{(D-3)/S}$. Since the AER recording system described in this article includes an anti-aliasing filter with a cutoff frequency of 3000 Hz and a steep slope of 24 dB per octave used in conjunction with a 16-bit AD/DA, the sampling rate must be over 22982 samples per second to avoid all aliasing errors. Hence, a sampling rate of 25 kHz could be appropriate to avoid all aliasing errors and at the same time, prevent undesired effects of oversampling.

2.2.4. Transducer

Earphones provide the stimulation of the auditory system of the subjects by transducing the electrical energy of the stimulation signal into acoustical energy (sound). The tubal insert earphones Etymotic ER3A (Etymotic Research, Inc., Elk Grove Village, IL) were chosen for this application because of their flat response on a wide band of frequencies, their isolation from external noise, and their fast response to typical click stimuli, which enables a synchronous firing of inner hair cells [13]. Other standard earphones such as the Telephonics TDH-39, -49, -50 (Cadwell Laboratories, Inc., Kennewick, WA) could also be used.

2.3. Software specifications

The software modules involved in the AERs recording process are presented in figure 6. The first step on data acquisition is the generation of the stimulation signal. The conventional stimulation technique consists of the presentation of stimuli with a constant inter-stimulus interval (ISI) greater than the averaging window to avoid overlapping responses [4]. Other more advanced methods can also be implemented to obtain AER at high stimulation rates such as maximum length sequences (MLS) [9], continuous loop averaging deconvolution (CLAD) [5,22], quasiperiodic sequence deconvolution (QSD) [18], least-squares deconvolution (LS) [2,3], and randomized stimulation and averaging (RSA) [27]. The stimulation of the auditory system is typically performed by 0.1 ms duration clicks in rarefaction polarity in order to evoke a synchronous firing of a large number of neurons [13]. Other types of stimuli can also be implemented such as tone bursts, filtered clicks, paired clicks, plops, chirps, modulated tones, stimulus trains, noise stimuli, and speech stimuli. The parameters type of stimuli, intensity level, clicks duration, clicks polarity, stimulation rate, and number of recorded sweeps can be controlled in this module. The “Stimulation & Recording” module consists of (a) the synchronous reproduction of the stimulation signal and (b) the synchronous recording of the stimulation signal and the digitized electroencephalogram (EEG). The user has the control of the number of quantization bits and the sampling rate on this step. The function of the “Scaling” module is to convert the recorded signal (A_X) into its corresponding value in microvolts at the electrodes. Considering G_A the gain of the amplifier for the band-pass frequencies and G_S the gain of the AD/DA, the scaled value in microvolts at the electrodes is $A_{scaled}(\mu V) = A_X \cdot \frac{1}{G_S} \cdot \frac{1}{G_A} \cdot 10^6$.

The values of G_A and G_S are estimated on the calibration process, which is described in section 2.4.1. The “AER enhancement” module incorporates algorithms to increase the quality of the response such as digital filtering and artifact rejection techniques. The “Synchronization” module uses the recording of the stimulation signal as trigger to determine the samples at which stimuli occurs. The “AER calculation” module runs the necessary algorithms to obtain the AER according to the method used in the stimulation process. This software module also compensates the phase distortion inserted by the analog filters of the amplifier on the recorded AER. Finally, the “Storage” module saves the raw data, the processed variables, and other important parameters into a file on the database. The parameters involved in the process of recording AERs can be managed from a graphical user interface (GUI). The structure of this multimedia platform can be designed according to the specific requirements of the users. Figure 7 shows an example of an interactive front-end of the AER recording system, in which the user has the control of recording parameters such as the interstimulus interval of the stimulation sequence (ISI), the number of recorded sweeps, the intensity level and the duration of the click. This platform also allows the use of specific signal processing techniques to obtain signals of higher quality such as digital filtering, frame rejection, and digital blanking. Additional information such as the number of accepted and rejected frames, the acceptance ratio, and the recorded EEG are also provided. In this example of front-end, the auditory evoked response is shown in a graph, as well as a history of previous recorded signals. An example of software routine that implements the recording of AER using the conventional method is available in MATLAB (The Mathworks, Inc., Natick, MA) code as supplementary material (Additional file).

2.4. Calibration

2.4.1. Calibration of G_A and G_S

The calibration process consists of estimating the values of the gain of the amplifier for the band-pass frequencies (G_A) and the gain of the AD/DA (G_S) to perform a correct scaling of the recording signal. The value of G_A can be estimated directly from the Bode diagram of the amplifier. The value of G_S is related to the intensity level of the input line of the AD/DA soundcard. This parameter can be configured from the audio settings of the laptop. Medium intensity level is recommended to avoid possible nonlinearities. The value of G_S can be estimated by correlating a recorded a signal whose maximum amplitude in volts is known (V_{hi}) with its corresponding value of the recorded signal (X_{hi}), $G_S = V_{hi} / X_{hi}$.

2.4.2. Calibration of the intensity level

The calibration of the intensity level consists of the measure of the stimulus magnitude, necessary for providing an accurate and uniform evaluation of the evoked responses. The standard audiometric calibration methods include dB normal hearing level (nHL) and dB sound pressure level (SPL) [6]. The intensity level 0 dB nHL represents the hearing threshold for normal hearing subjects. This intensity level can be established as the mean value of the intensity level at which stimuli are just detectable in a set of 15 to 20 subjects with no auditory dysfunction (normal hearing subjects) [13]. The intensity level of a stimulus in terms of dB SPL is estimated as $20 \cdot \log_{10}\left(\frac{P_x}{P_{ref}}\right)$, being P_x the pressure of the stimulus and P_{ref} the reference pressure, whose typical reference value is 20 μPa. A complete description of the procedure to calibrate the reference zero is described by the international standard ISO 389 [15,25]. In this system, the calibration of the stimuli is performed according to the aforementioned international standard. The intensity level can be controlled by the user through the output voltage of the stimulation signal. Given V_{ref} as the amplitude voltage of a stimulation signal that presents an intensity level of 0 dB nHL, the amplitude voltage necessary to present an intensity level of X dB nHL can be obtained according to: $V_X = V_{ref} \cdot 10^{X/20}$.

2.5. Scalability

The use of multiple-channel systems might be required in certain research applications, e.g., the use of binaural stimulation for simultaneous screening in both ears, the use of contralateral masking to ensure monaural stimulation, and the simultaneous screening of ABR and electrocochleography (ECochG) [24]. The AER recording system described in this system is scalable. A multichannel version of this system can be set up using an AD/DA converter of multiple channels, and multiple units of the amplifier. Considering that the price of a standard 4 channels AD/DA sound card is about 150 USD, and that the rough manufacturing cost of an amplifier unit is about 200 USD, the implementation of a 4 channels AER recording system would reach a total manufacturing cost of about 1250 USD.

3. ASSESSMENT

The performance of the AER recording system described in this article is evaluated by a number of experiments conducted on one normal hearing subject (#S1: male, 28 yr). The subject explored in these experiments was informed about the experimental procedure and possible side effects of the test, and gave consent for the use of the data. The calibration of the intensity level was carried out according to the international standard ISO 389 [15,25]. The equivalent 0 dB nHL corresponds to 36.4 dB SPL. The recording procedure of these experiments was approved by the Clinical Research Ethics Committee of the San Cecilio University Hospital and by the Human Research Ethics Committee of the University of Granada (Reference No. 826014263-14263-4-9), in accordance with the Code of Ethics of the World Medical Association (Declaration of Helsinki) for experiments involving humans. Additionally, this section introduces an outline of related research activities carried out by the AER recording system described in this paper.

Experiment 1 was driven to simulate the recording of ABR and MLR signals and assess the performance of the AER recording system. The ABR and MLR signals used in this experiment (original pseudopotentials) were obtained from #S1 using 10.000 click stimuli presented at a rate of 33 Hz for ABR and 3.3 Hz for MLR at an intensity level of 70 dB nHL. A burst of 10.000 pseudopotentials was digitally synthesized for each type of signal. The amplitude of both signals was reduced by a voltage divider to obtain signals of 0.2 μV for ABR and 0.5 μV for MLR. The burst of low-amplitude pseudopotentials was amplified, recorded by the AD/DA soundcard, and digitally processed according to the recording procedure described in section II. Figure 8 shows the original and recorded pseudopotentials for ABR and MLR signals. The most important components of these signals are marked on the figure. This figure shows that the AER recording system described in this article can be used to obtain signals similar in morphology and amplitude to ABR and MLR since the major components of these signals can be easily identified, remain on the same latency, and present similar amplitude.

Experiment 2 analyzes the effects of noise reduction through sweeps averaging. Figure 9 shows ABR and MLR signals obtained from #S1 at a different number of averaged sweeps. The stimuli used on this experiment were clicks presented at 70 dB nHL at a stimulation rate of 33 Hz for ABR and 8 Hz for MLR. This figure shows that the quality of the AER increases with the number of averaged sweeps. The main waves of these signals start to be identified with at least 500 sweeps. The recordings obtained with 20.000 sweeps are of a high quality but require a long test time, especially for MLR signals. A number of 2000 sweeps can be found appropriate to reach a compromise between recording time and quality of the recordings. However, the recording of AER obtained with larger number of averaged sweeps can be interesting in certain applications, such as the study of neural adaptation, that require the analysis of high quality AER and do not impose significant restrictions on the recording test time [34].

Experiment 3 evaluates the influence of intensity level on the morphology of ABR signals. Figure 10 shows ABR signals from #S1 obtained at intensity levels of stimulation that vary from 5 to 80 dB nHL, in steps of 5 dB. 5.000 sweeps were recorded for each ABR signal. Waves I, III, and V are labeled on the ABR signal obtained at 80 dB nHL. This experiment shows that the amplitude of the most relevant waves decreases and their corresponding latency increases as the stimulation intensity level decreases. Wave V remains as the most robust component, that in this experiment can be clearly identified up to 15 dB nHL. These results are in accordance with previous literature [14,17].

Experiments 4 and 5 analyze the effects of stimulation rate on the morphology of ABR and MLR signals respectively. Figure 11 shows ABR signals from #S1 obtained at stimulation rates up to to 250 Hz using the randomized stimulation and averaging (RSA) [27], the quasiperiodic sequence deconvolution (QSD) [18], and the conventional (CONV) techniques [4]. All recordings were obtained using 5.000 averaged sweeps stimulated with clicks at 70 dB nHL. The amount of jitter used in the stimulation sequences for RSA and QSD was 4 ms. The jitter of a stimulation sequence measures the grade of dispersion of the ISI compared to a periodical presentation of the stimuli, i.e., the ISI of stimuli presented at a rate of 25 Hz with a jitter of 4 ms would vary between 38 and 42 ms.

Both RSA and QSD techniques are valid methods to obtain ABR signals at very high stimulation rates (greater than 100 Hz). Waves I, III, and V can be clearly identified in all recordings, although the ABR signal obtained with QSD at 250 Hz is slightly noisier. This figure shows the normal changes on the morphology of the ABR as stimulation rate increases: amplitude of waves decrease and latencies increase, with a deeper shift on the most central waves. Figure 12 shows MLR signals from #S1 obtained at stimulation rates from 8 to 125 Hz obtained with the RSA technique with a jitter of 16 ms, using click stimuli presented at 70 dB nHL. The V, Na, Pa, Nb, Pb components can be identified at all stimulation rates. These components are labeled on the MLR signal obtained at 125 Hz. The MLR signal obtained at 40 Hz presents a resonance, in which the Na, Pa, Nb, and Pb components are in phase (occur at the same time relative to the stimulus) and become superimposed. This phenomenon is generally known as 40-Hz event-related potential (ERP) and was first described by Galambos et al. (1981) [10]. The 40-Hz ERP presents advantages for the estimation of the auditory threshold due to its large amplitude (usually greater than 1 μV).

In addition to these five experiments, the AER recording system described in this paper has been successfully used in related research activities. This system was used to develop (a) the RSA method, a technique that allows the recording of AER at high rates [27]; the separated response method, which allowed for the first time the study of the fast and slow mechanisms of adaptation in humans [29,34]; (c) the fitted parametric peaks (FPP) method, which provides an automatic evaluation of the quality of ABR signals and a parameterization of the most important waves in terms of amplitude, latency and width [30,35]; (e) studies to test whether or not high stimulation rates could save recording time [28,36]; (f) an automatic auditory response detection paradigm based on response tracking [31]; (g) a study of the effects of averaging and deconvolution in ABR and MLR signals using the RSA method [32]; and (h) a deconvolution method based on randomized stimulation using artifact rejection methods in the frequency domain [33].

4. DISCUSSION

This paper provides a full description of a flexible, high-performance, and inexpensive auditory evoked response recording system. The system described in this article includes an amplifier, an external sound card that acts as an AD/DA converter of two I/O channels, electrodes, cables and connectors, and a laptop with software modules that run the algorithms for the stimulation sequence generation, the production of the stimuli and the recording of the sweeps, the scaling of the recorded EEG, the synchronization of the sweeps with their associated stimuli, the processing of data according to the specific stimulation method to obtain the AER (conventional, MLS, QSD, CLAD, LS, RSA, etc.), and finally, the storage of the EEG and the AER into a file.

The open nature of this system provides the flexibility required on many research applications. Almost every parameter involved in the AER recording process could be defined and controlled. For instance, this system gives the user the control on parameters such as the nature, duration and polarity of stimuli, the number of averaged sweeps, the intensity level, and the stimulation rate. The software platform of this system allows the implementation of advanced stimulation methods, such as RSA and QSD, which allows the recording of AER signals at high rates of stimulation, digital filtering to enhance the quality of the recordings, and the use of artifact rejection methods. In addition, the recording of the raw electroencephalogram may be of interest to implement advanced signal processing methods offline. Furthermore, the scalability of the system allows the implementation of a multiple-channel design, which might be useful in certain research applications such as the use of binaural stimulation for simultaneous screening in both ears, the use of contralateral masking to ensure monaural stimulation, and the simultaneous screening of ABR and electrocochleography (ECochG) [24].

The performance of this system was evaluated through a number of experiments that include (a) the recording of artificially synthesized ABR and MLR signals (pseudopotentials), (b) the recording of real ABR and MLR signals of different quality using a varying number of averaged sweeps, (c) the analysis of the influence of the intensity level on the morphology of ABR signals, (d) and the study of the effects of stimulation rate on the morphology of ABR and MLR signals. Some of the results obtained in these experiments are especially remarkable, such as the ABR signal obtained at 250 Hz and the MLR signal recorded at 125 Hz (experiments 4 and 5). In addition to these experiments, the AER recording system proposed in this article has been proven to be effective in several preceding studies, e.g., this architecture was used (a) to develop the RSA method and compare its performance with the QSD technique through ABR signals recorded from 8 subjects at different stimulation rates [27]; (b) to do a study of the fast and slow mechanisms of adaptation in humans by analyzing the morphology of ABR signals obtained with the separated responses methodology [29,34]; (c) to develop and evaluate different approaches of automatic quality assessment and response detection methods [30,31,35]; (d) to carry out a study to test whether or not high stimulation rates could save recording time [28,36]; (e) an analysis of the effects of adaptation and deconvolution of ABR and MLR signals with RSA [32]; and (f) to develop a method that allows the deconvolution of overlapping responses with randomized stimulation using frequency domain-based artifact rejection methods [33]. The analysis of the results of the experiments carried out in this article along with the results obtained in the aforementioned preceding studies [27-36], point out that the AER recording system described in this article can be efficiently used to record ABR and MLR signals in different recording conditions.

Despite already exist several clinical devices for recording AERs, most of them are expensive and suffer from a lack of flexibility since they are designed for specific applications (e.g., hearing threshold estimation). The commercial systems designed for research applications are more flexible than the aforementioned clinical devices; however, the flexibility of these systems is limited by the performance of their associated software, and their acquisition price is usually high since it includes not only the cost of the materials, but also costs derived from marketing, distribution, technical support, profit margin, etc. In contrast, the rough cost for the implementation of a prototype of the described AER recording system including circuitry, connectors, box, external AD/DA soundcard, the Etymotic ER·3A insert earphones, electrodes, and cables (laptop not included) is less than 1000 USD. The cost-efficient nature of the auditory evoked response recording system described in this article, along with its high-performance and flexibility, could be valuable in several research applications in Audiology.

5. CONCLUSION

This article describes in detail the hardware and software elements of an auditory evoked response recording system. The performance of this system has been assessed by five experiments with both real and artificially synthesized ABR and MLR signals in different recording conditions. The high-performance, flexible, and cost-efficient nature of the AER recording system described in this article could be valuable in several research applications in the field of Audiology.

ADDITIONAL FILE

Additional file 1: Example of MATLAB routine that implements the recording of AER using the conventional method.

COMPETING INTERESTS

There are no conflicts of interest associated with this research article. The authors have no financial involvement or interest with any organization or company about subjects or materials discussed in the paper.

ACKNOWLEDGMENT

This research is granted by the project “Design, implementation and evaluation of an advanced system for recording Auditory Brainstem Response (ABR) based in encoded signaling” (TEC2009-14245), R&D National Plan (2008-2011), Ministry of Economy and Competivity (Government of Spain) and “European Regional Development fund Programme” (2007-2013); by the “Granada Excellence Network of Innovation Laboratories - Startup Projects for Young Researchers Programme” (GENIL-PYR 2014), Campus of International Excellence, Ministry of Economy and Competitivity (Government of Spain); and by the grant “Formación de Profesorado Universitario” (FPU) (AP2009-3150), Ministry of Education, Culture, and Sports (Government of Spain).

REFERENCES

[1] Bahmer A, Peter O, Baumann U. Recording of electrically evoked auditory brainstem responses (E-ABR) with an integrated stimulus generator in Matlab. J Neurosci Meth 2008; 173: 306-314.

[2] Bardy F, Dillon H, Van Dun B. Least-squares deconvolution of evoked potentials and sequence optimization for multiple stimuli under low-jitter conditions. Clin Neurophysiol 2014; 125: 727-737.

[3] Bardy F, Van Dun B, Dillon H, McMahon. Deconvolution of overlapping cortical auditory evoked potentials recorded using short stimulus onset-asynchrony ranges. Clin Neurophysiol 2014; 125: 814-826.

[4] Dawson GD. A summation technique for the detection of small evoked potentials. Electroencephalogr Clin Neurophysiol 1954; 6: 65-84.

[5] Delgado RE, Özdamar O. Deconvolution of evoked responses obtained at high stimulus rates. J Acoust Soc Am 2004; 115: 1242-1251.

[6] Durrant JD, Boston JR. Stimuli for auditory evoked potential assessment. In: Sabatini P, Klinger AM, Ajello JP, editors. Auditory Evoked Potentials. Basic principles and clinical application. Baltimore: Lippincott Williams & Wilkins 2007: 42-72.

[7] Eggermont JJ. Electric and magnetic fields of synchronous neural activity. In: Sabatini P, Klinger AM, Ajello JP, editors. Auditory Evoked Potentials. Basic principles and clinical application. Baltimore: Lippincott Williams & Wilkins 2007: 2-21.

[8] Elberling C, Don M. Detecting and assessing synchronous neural activity in the temporal domain (SNR, Response detection). In: Sabatini P, Klinger AM, Ajello JP, editors. Auditory Evoked Potentials. Basic principles and clinical application. Baltimore: Lippincott Williams & Wilkins 2007: 102-123.

[9] Eysholdt U, Schreiner C. Maximum length sequences: A fast method for measuring brain-stem-evoked responses. Audiol 1982; 21: 242-250.

[10] Galambos R, Makeig S, Talmachoff PJ. A 40-Hz auditory potential recorded from the human scalp. P Natl Acad Sci USA 1981; 78: 2643-2647.

[11] Gravaill N. A simple battery-operated a.c. impedance meter. Med Biol Eng Comput 1978; 16: 339-340.

[12] Grimnes S. Impedance measurement of individual skin Surface electrodes. Med Biol Eng Comput 1983; 21: 750-755.

[13] Hall JW. New handbook of Auditory Evoked Responses. 1st ed. Boston: Pearson Allyn and Bacon; 2007.

[14] Hecox K, Galambos R. Brain stem auditory evoked responses in human infants and adults. Arch Otolaryngol 1974; 99: 30-33.

[15] ISO 389-x. Acoustics – Reference zero for the calibration of audiometric equipment – Part 1-9. International Organization for Standard.

[16] Jasper HH. The ten-twenty electrode system of the International Federation. Electroencephalogr Clin Neurophysiol 1958; 10: 371-375.

[17] Jewett DL, Williston JS. Auditory-evoked far fields averaged from the scalp of humans. Brain 1971; 94: 681-696.

[18] Jewett DL, Caplovitz G, Baird B, Trumpis M, Olson MP, Larson-Prior LJ. The use of QSD (q-sequence deconvolution) to recover superposed, transient evoked-responses. Clin Neurophysiol 2004, 115: 2754-2775.

[19] Jurcak V, Tsuzuki D, Dan I. 10/20, 10/10, and 10/5 systems revisited. Their validity as relative head-surface-based positioning systems. Neuroimage 2007; 34: 1600-1611.

[20] Lasky RE. Rate and adaptation effects on the auditory evoked brainstem response in human newborns and adults. Hearing Res 1997; 111: 165-176.

[21] Nyquist H. Certain factors affecting telegraph speed. Bell Syst Tech J 1924; 3: 324-346.

[22] Ozdamar O, Bohorquez J. Signal-to-noise ratio and frequency analysis of continuous loop averaging deconvolution (CLAD) of overlapping evoked potentials. J Acoust Soc Am 2006; 119: 429-438.

[23] Ozdamar O, Bohorquez J, Ray SS. Pb(P1) resonance at 40 Hz: Effects of high stimulus rate on auditory middle latency responses (MLRs) explored using deconvolution. Clin Neurophysiol 2007; 118: 1261-1273.

[24] Reid A, Thornton ARD. The effects of contralateral masking upon brainstem electric responses. Brit J Audiol 1983; 17: 155-162.

[25] Richter U, Fedtke T. Reference zero for the calibration of audiometric equipment using ‘clicks’ as test signals. Int J Audiol 2005; 44: 478-487.

[26] Thornton ARD. Instrumentation and Recording Parameters. In: Sabatini P, Klinger AM, Ajello JP, editors. Auditory Evoked Potentials. Basic principles and clinical application. Baltimore: Lippincott Williams & Wilkins 2007: 73-101.

[27] Valderrama JT, Alvarez I, de la Torre A, Segura JC, Sainz M, Vargas JL. Recording of auditory brainstem response at high stimulation rates using randomized stimulation and averaging. J Acoust Soc Am 2012; 132: 3856-3865.

[28] Valderrama JT, Alvarez I, de la Torre A, Segura JC, Sainz M, Vargas JL. Reducing recording time of brainstem auditory evoked responses by the use of randomized stimulation. Newborn Hearing Screening Congress, June 5-7 2012, Cernobbio (Como Lake), Italy.

[29] Valderrama JT, Alvarez I, de la Torre A, Segura JC, Sainz M, Vargas JL. A preliminary study of the short-term and long-term neural adaptation of the auditory brainstem response by the use of randomized stimulation. Adults Hearing Screening Congress, June 7-9 2012, Cernobbio (Como Lake), Italy.

[30] Valderrama JT, Alvarez I, de la Torre A, Segura JC, Sainz M, Vargas JL. A portable, modular, and low cost auditory brainstem response recording system including an algorithm for automatic identification of responses suitable for hearing screening. IEEE/EMBS Special Topic Conference on Point-of-Care (POC) Healthcare Technologies: Synergy Towards Better Global Healthcare, January 16-18 2013, Bangalore, India. PHT 2013; art. no. 6461314, 180-183.

[31] Valderrama JT, Morales JM, Alvarez I, de la Torre A, Segura JC, Sainz M, Vargas JL. Automatic quality assessment and response detection of auditory evoked potentials based on response tracking. XXIIIrd

International Evoked Response Audiometry Study Group (IERASG) Symposium, June 9-13 2013, New Orleans, LA: 55.

[32] Valderrama JT, de la Torre A, Alvarez I, Segura JC, Sainz M, Vargas JL. Auditory middle latency responses recorded at high stimulation rates using randomized stimulation and averaging. XXIIIrd International Evoked Response Audiometry Study Group (IERASG) Symposium, June 9-13 2013, New Orleans, LA: 56.

[33] Valderrama JT, de la Torre A, Alvarez I, Segura JC, Sainz M, Vargas JL. Deconvolution of overlapping responses and frequency domain-based artifact rejection methods using randomized stimulation. XXIIIrd International Evoked Response Audiometry Study Group (IERASG) Symposium, June 9-13 2013; New Orleans, LA: 57.

[34] Valderrama JT, de la Torre A, Alvarez I, Segura JC, Thornton ARD, Sainz M, Vargas JL. A study of adaptation mechanisms based on ABR recorded at high stimulation rate. Clin Neurophysiol 2014; 125: 805-813.

[35] Valderrama JT, de la Torre A, Alvarez I, Segura JC, Thornton ARD, Sainz M, Vargas JL. Automatic quality assessment and peak identification of auditory brainstem responses with fitted parametric peaks," Comput Meth Prog Bio 2014; 114: 262-275.

[36] Valderrama JT, de la Torre A, Alvarez I, Segura JC, Kaf W, Sainz M, Vargas JL. A more efficient use of the recording time with randomized stimulation and averaging (RSA) in hearing screening applications. 9th

International Conference of the Saudi Society of Otorhinolaryngology – Head and Neck Surgery, March 4-6 2014, Riyadh, Kingdom of Saudi Arabia.

[37] Wong PKH, Bickford RG. Brain stem auditory evoked potentials: the use of noise estimate. Electroencephalogr Clin Neurophysiol 1980; 50: 25-34.

[38] (2012) Medical Electrical Equipment – Part 1: General Requirements for Basic Safety and Essential Performance. International Electrotechnical Commission IEC 60601-1.

Figure legends:

- Figure 1. General scheme of the AER recording system.
- Figure 2. Picture of the electronics of the amplifier (left) and hardware modules of the AER recording system (right).
- Figure 3. Electronic circuit diagram of the amplifier.
- Figure 4. Bode diagram of the amplifier.
- Figure 5. Input signal versus output signal graph for a linearity analysis of the ABR amplifier.
- Figure 6. Software modules diagram.
- Figure 7. Interactive front-end of the AER recording system. This multimedia platform allows the user a full control of all parameters involved in the AER recording process.

- Figure 8. Recording of low-amplitude digitally synthesized signals similar in morphology to ABR and MLR potentials.
- Figure 9. Influence of the number of averaged sweeps on the quality of ABR and MLR signals.
- Figure 10. ABR signals obtained at different intensity levels of stimulation.
- Figure 11. ABR signals recorded at different stimulation rates using the randomized stimulation and averaging (RSA), the quasiperiodic sequence deconvolution (QSD), and the conventional (CONV) methods.
- Figure 12. MLR signals obtained at different stimulation rates using the randomized stimulation and averaging (RSA) technique.

Table legends:

- Table 1. Rough cost analysis of the elements that compose the AER recording system.
- Table 2. Frequency bandwidth of different AERs and suggested values of resistors and capacitances that implement the high pass and low pass filtering stages of the amplifier.
- Table 3. Features of the AD/DA soundcard.

Supplementary Material

Example of MATLAB routine that implements the recording of AER using the conventional method

```
%% PARAMETERS INITIALIZATION
fs = 25e3;                      % Sampling rate
Name_File = 'EEG_Example';      % Name of the file
ER = 1;                         % Evoked response: ER=0 for ABR, ER=1 for
MLR
if(ER)
    window = 12e-3;             % Time window of 12 ms for ABR
    Low_freq = 100;             % Low-pass frequency for digital filter
    High_freq = 3000;           % High-pass frequency for digital filter
    Phase_delay = 15;           % Phase distortion compensation (560 us)
else
    window = 100e-3;            % Time window of 100 ms for MLR
    Low_freq = 10;              % Low-pass frequency for digital filter
    High_freq = 3000;           % High-pass frequency for digital filter
    Phase_delay = 3;            % Phase distortion compensation (80 us)
end
AER = zeros(window*fs,1);       % AER initialization
ISI = 0.030;                    % Interstimulus interval of the sequence
in ms
N_Sweeps = 2000;                % Number of recorded sweeps
Click_Duration = 120e-6;        % Duration of the click in s
Ga = 1250;                      % Gain of the amplifier (calib)
Gs = 1.0461;                    % Gain of the AD/DA soundcard (calib)
Filter_Order = 4;               % Order of the digital filters
V_ref = 9.8465e-5;              % Absolute intensity level for 0 dBnHL
(calib)
I = 70;                         % Intensity level in dBnHL
clear ER window

%% STIMULATION SIGNAL GENERATION
x(1:Click_Duration*fs,1) = -1;            % Pattern of the rarefaction
click
h(1:ISI*fs:N_Sweeps*ISI*fs) = 1;          % h=1 -> start of the stimuli
Seq = conv(x,h);                          % Signal sequence generation
% Channel 1 - Stimulation signal. Channel 2 - Synchronization signal
Seq(:,2) = Seq(:,1);                      % 2-channels sequence
t_blocking = floor(length(Seq)/fs);       % Recording test time
Seq(:,1) = Seq(:,1)*V_ref*10^(I/20);      % Seq - intensity level
calibrated
clear Click_Duration N_Sweeps ISI x h V_ref I

%% STIMULATION & RECORDING
x = audioplayer(Seq,fs,16);
play(x);
sound(Seq,fs,16);
recorder = audiorecorder(fs,16,2);
recordblocking(recorder,t_blocking);
y = getaudiodata(recorder);
clear t_blocking Seq x recorder

%% SCALING
```

```
EEG = y(:,1)-mean(y(:,1));          % Remove the offset of the input signal
EEG = EEG/Ga/Gs*1e6;                % EEG calibrated in microvolts
Sinc = y(:,2)-mean(y(:,2));         % Remove the offset of the input signal
clear y Ga Gs

%% AER ENHANCEMENT
[b a] = butter(Filter_Order,[Low_freq High_freq]*2/fs,'bandpass');
Resp = filter(b,a,EEG);             % EEG after digital filtering
clear a b Filter_Order Low_freq High_freq

%% SYNCHRONIZATION
% Sinc is replaced with samples of amplitude over the 70% of the maximum
Sinc = find(Sinc>0.7*max(Sinc));
% Only the first sample is relevant. The following 10 samples are removed.
m(1) = Sinc(1);                     % m(j) - Synchronization samples
j = 1;
for i=2:size(Sinc,1)-10
    if((Sinc(i)-m(j))>10)
        j = j+1;
        m(j) = Sinc(i);
    end
end
NN = length(m);                     % NN is the number of recorded sweeps
clear Sinc i j

%% AER CALCULATION
for i=1:NN
    AER = AER + Resp(m(i):m(i)+length(AER)-1)/NN;  % Sweeps averaging
end
AER = AER(Phase_delay:length(AER)); % Phase distortion compensation
clear i

%% STORAGE
save(Name_File,'AER','EEG','m','NN','fs');
fprintf('Data in <%s.mat>\n',Name_File);
```

Table 1.

Element	Rough cost
Amplifier electronics[1]	200 USD
Electrodes and electrolytic paste	200 USD
Etymotic ER·3A insert earphones	500 USD
External AD/DA sound card	50 USD
TOTAL	950 USD

[1] Amplifier electronics include semiconductor elements, integrated circuits, connectors, PCB card, box, batteries, and battery holders.

Table 2.

Evoked response	Bandwidth	High pass filter				Low pass filter			
		R1-H	R2-H	C1-H	C2-H	R1-L	R2-L	R1-H	R1-H
ABR	[150 3500]	33kΩ	33kΩ	47nF	22nF	6.8kΩ	6.8kΩ	4.7nF	10nF
MLR	[0.5 3500]	1MΩ	1MΩ	470nF	470nF	6.8kΩ	6.8kΩ	4.7nF	10nF

Table 3.

Feature	Value
Sampling rate	25 kHz
Input range	-3 V / +3 V
Output range	-2.5 V / +2.5 V
Bits of quantization	16
Quantization step	91.55 μV

Figure 1

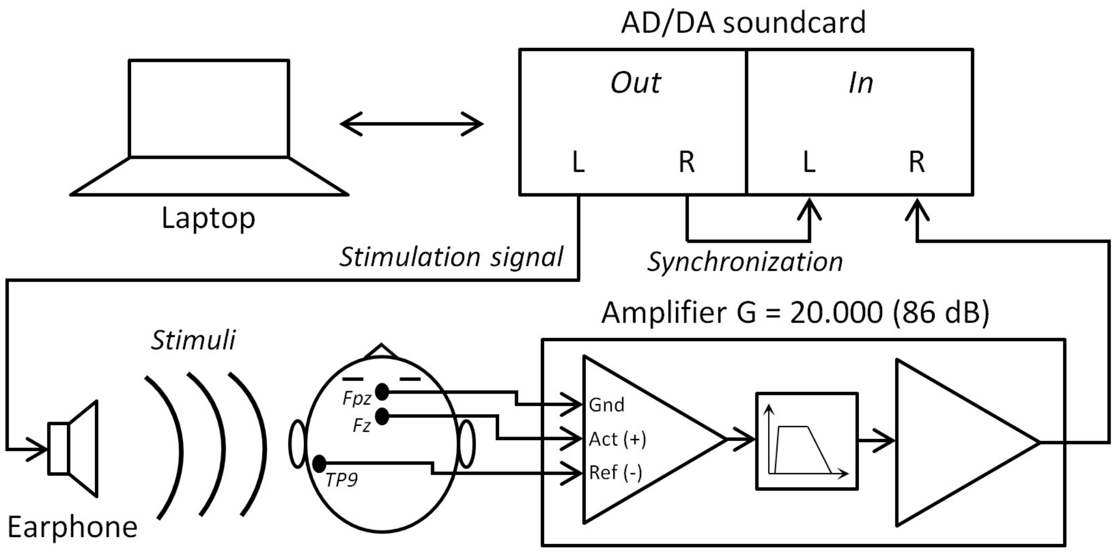

Figure 2

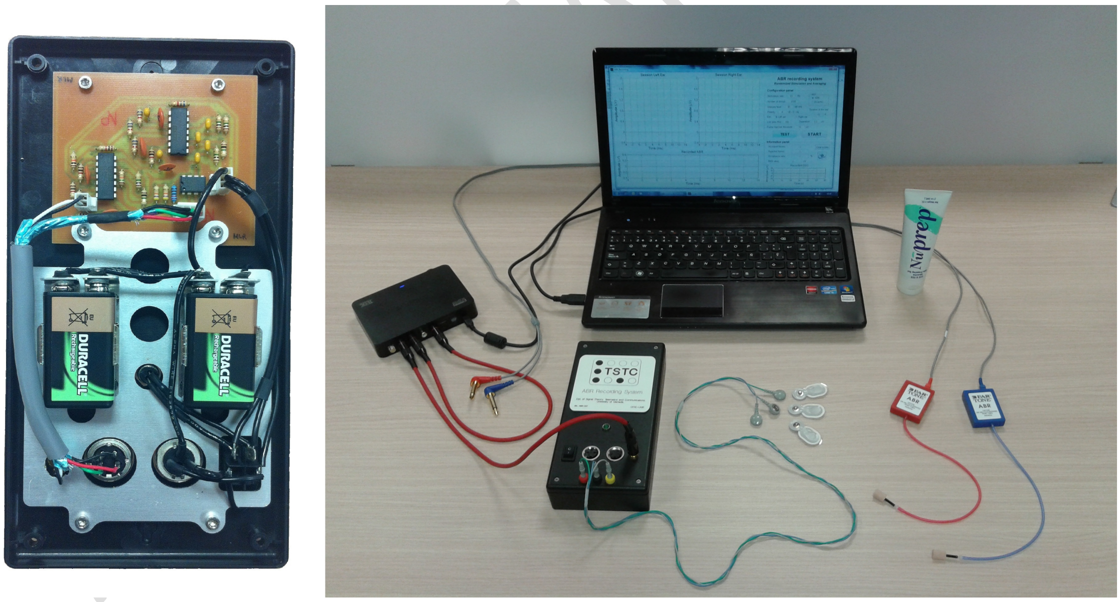

Figure 3

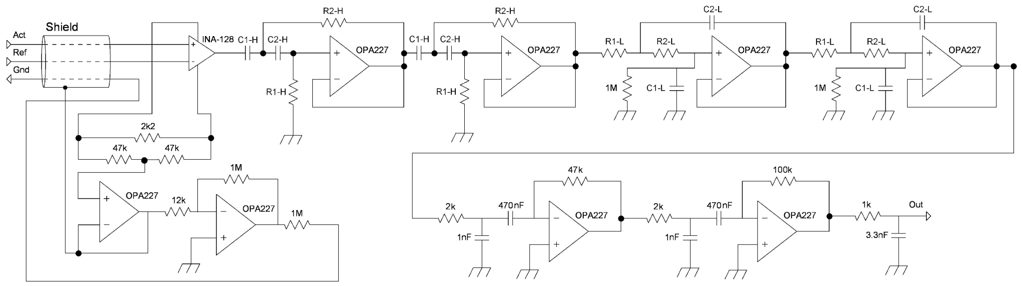

Figure 4

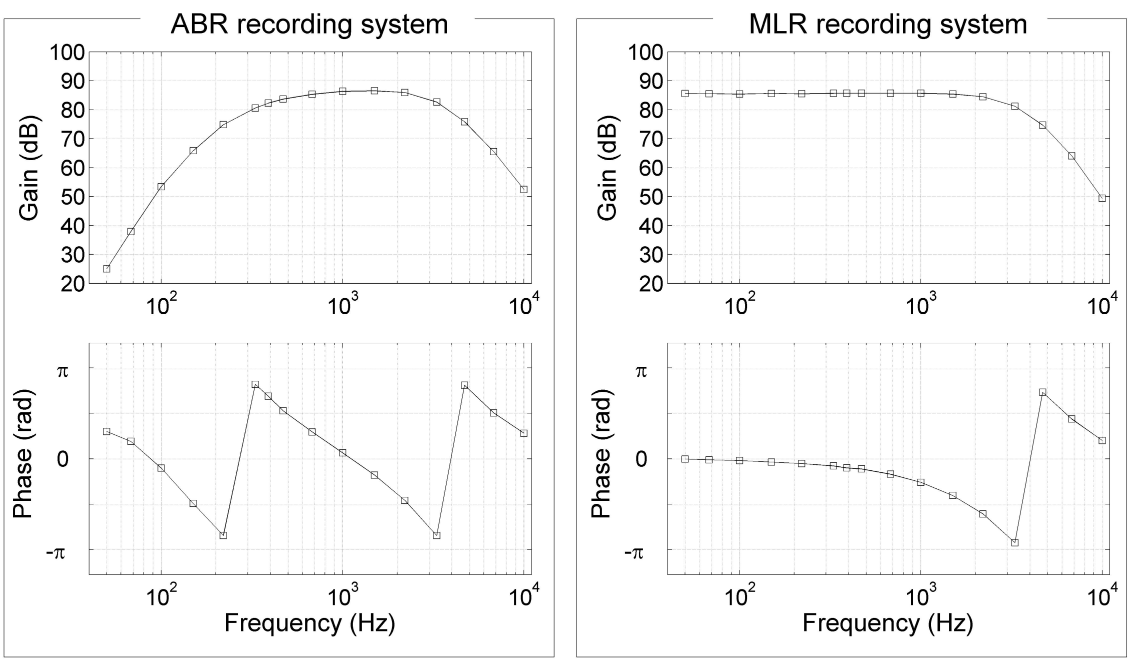

Figure 5

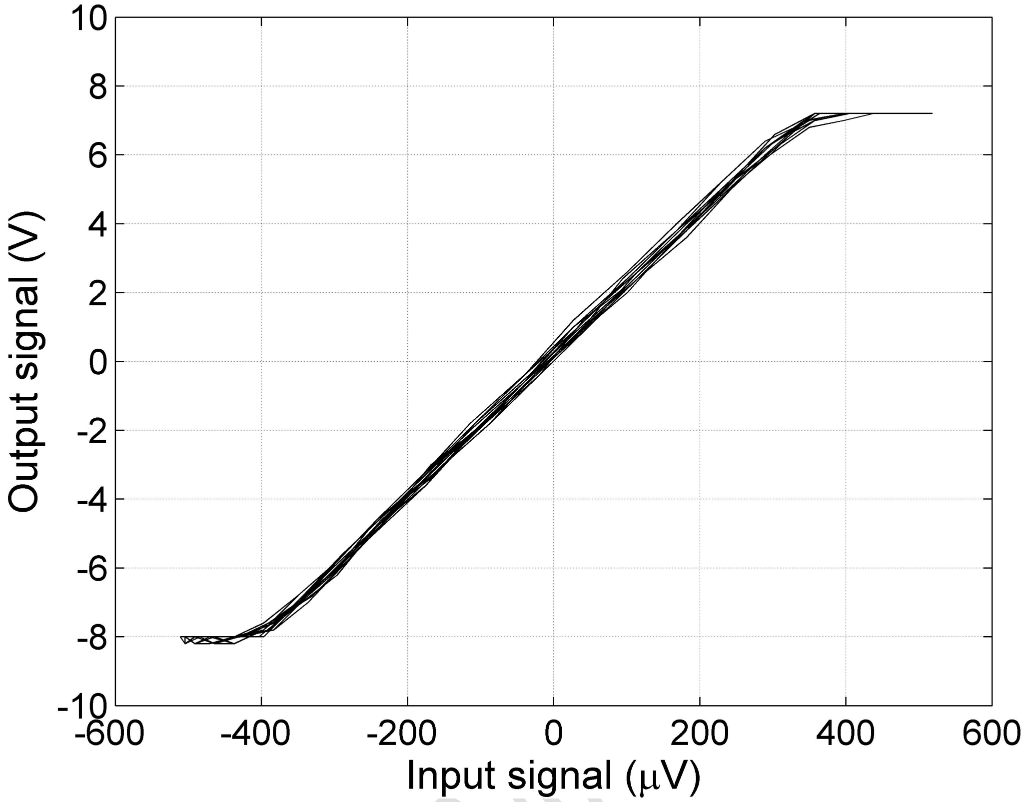
10
8
6
4
2
0
-2
-4
-6
-8
-10
Output signal (V)
-600
-400
-200
0
200
400
600
Input signal (μV)

Figure 6

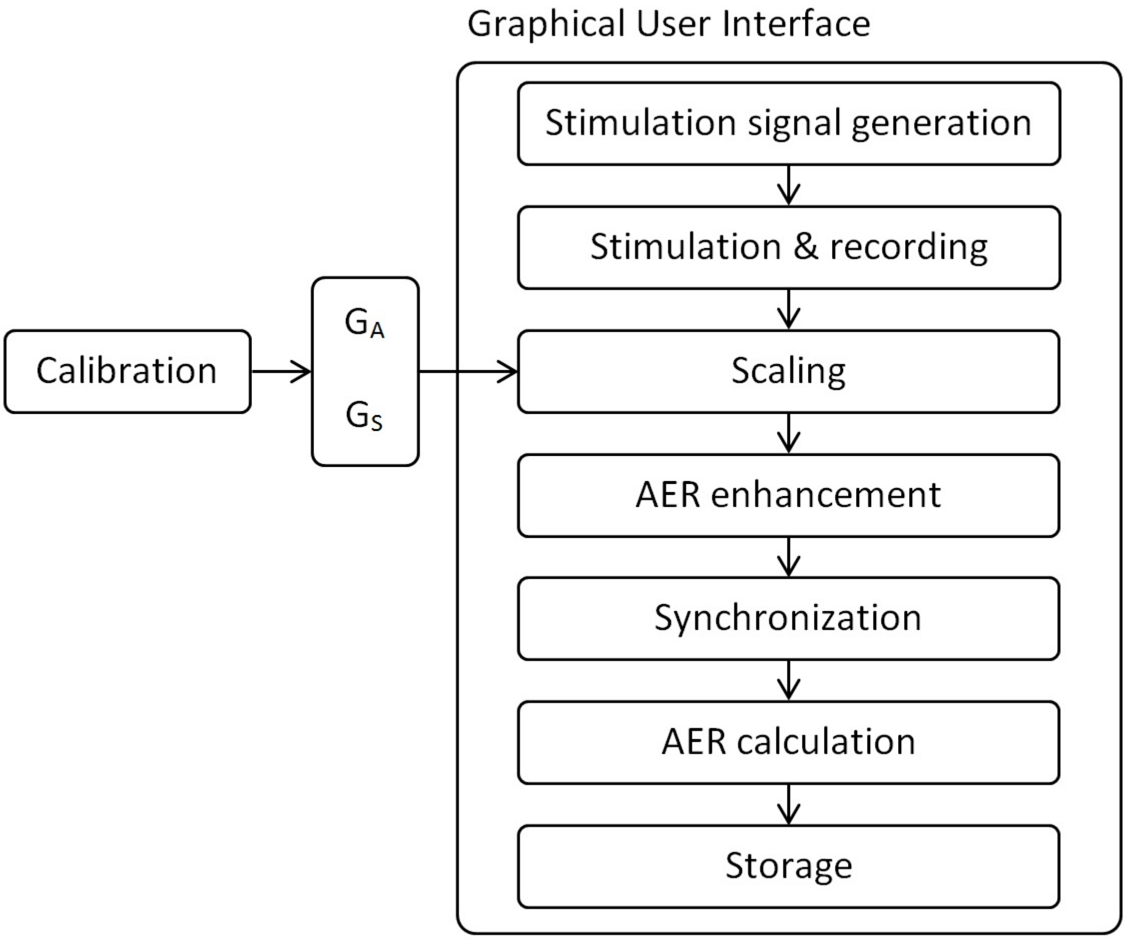

Figure 7

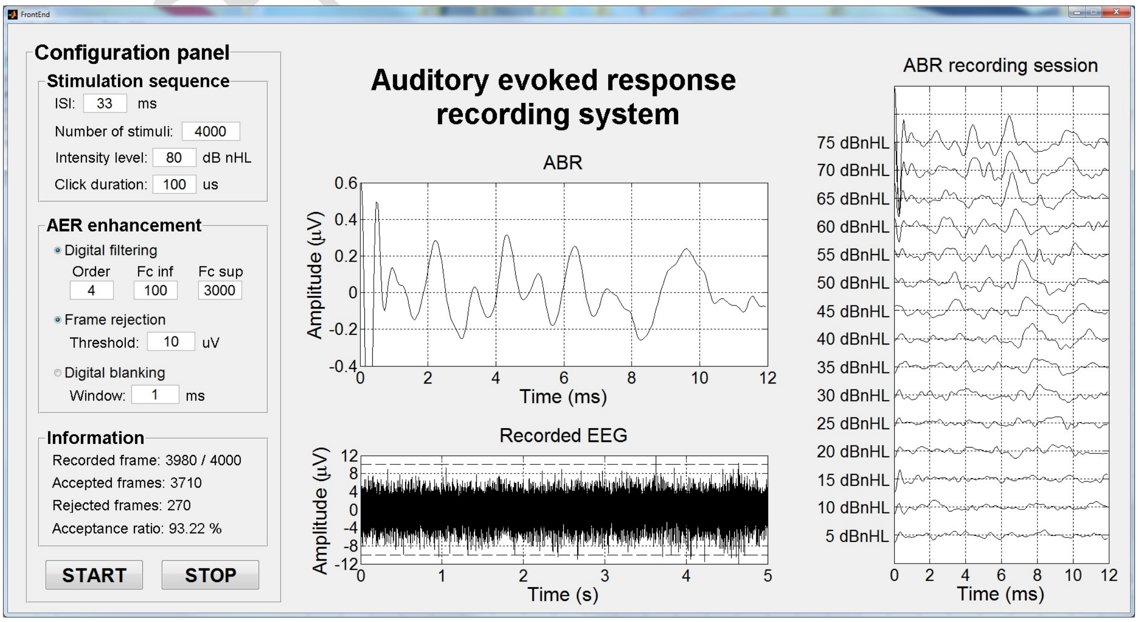

Figure 8

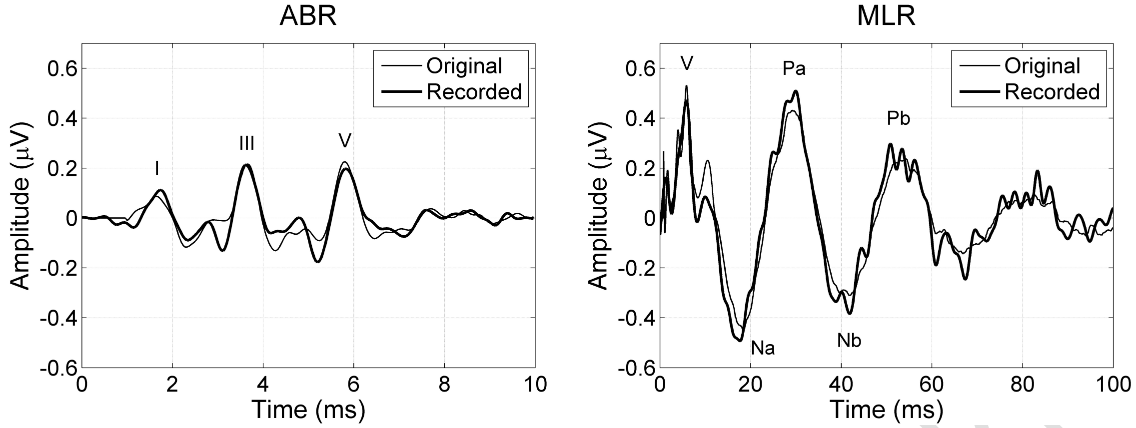

Figure 9

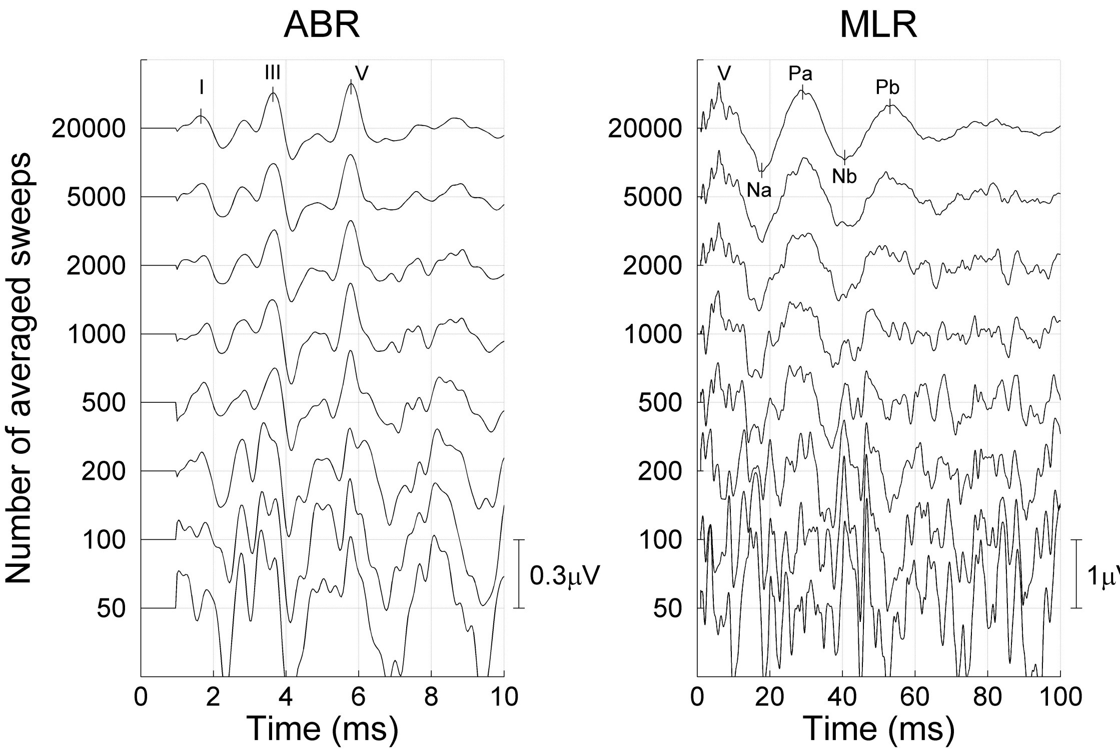

Figure 10

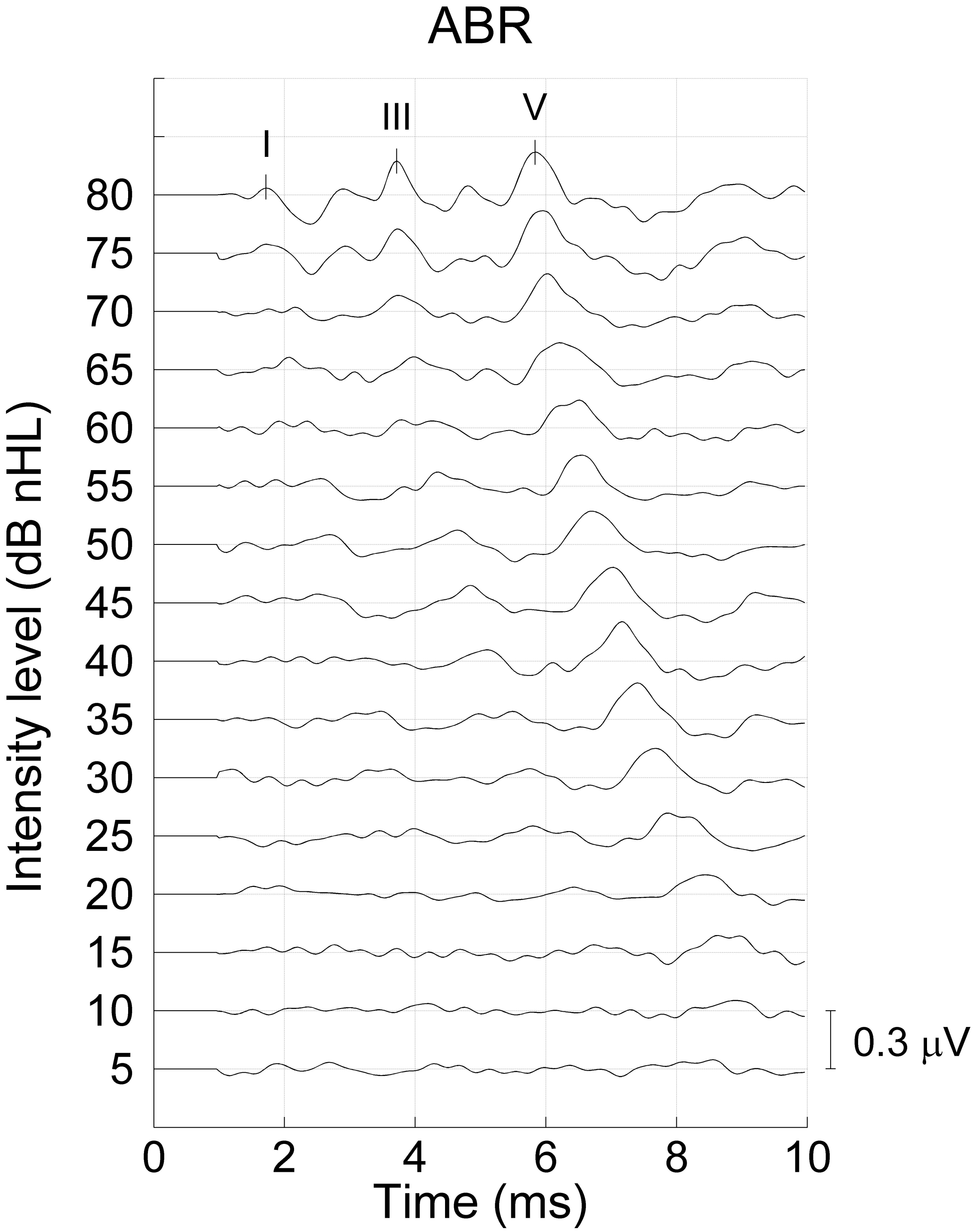
ABR
I
III
V
80
75
70
65
60
55
50
45
40
35
30
25
20
15
10
5
Intensity level (dB nHL)
0.3 μV
0
2
4
6
8
10
Time (ms)

Figure 11

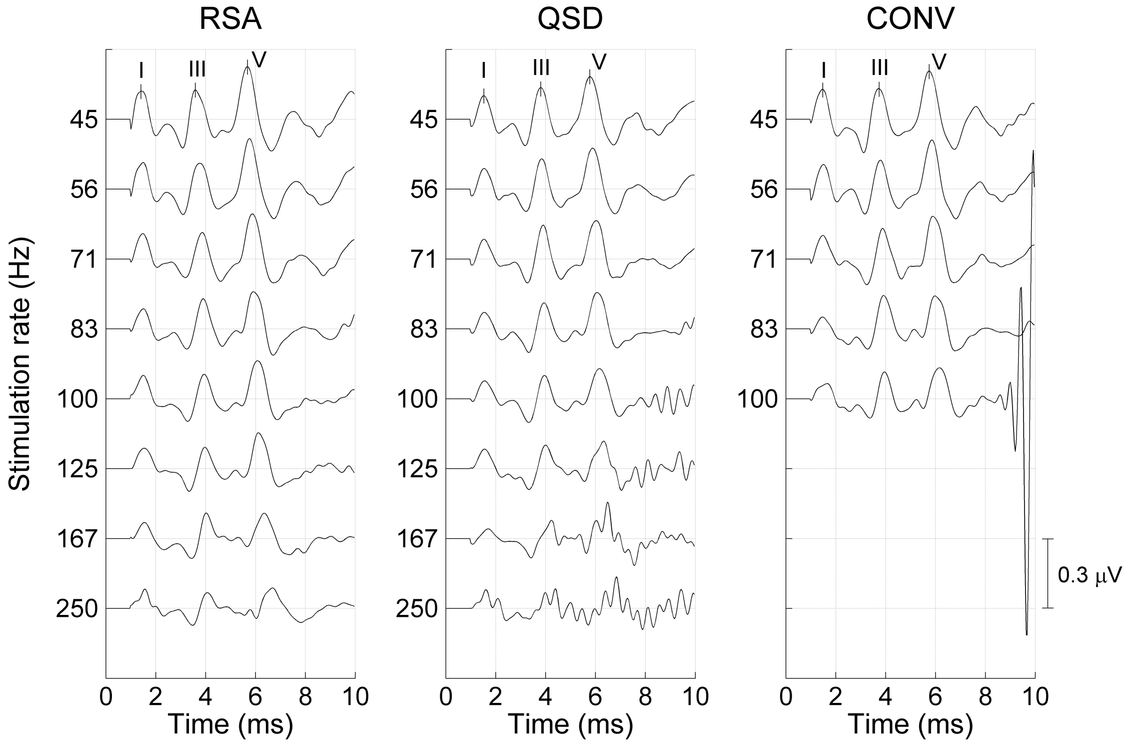
RSA
QSD
CONV
I
III
V
Stimulation rate (Hz)
45
56
71
83
100
125
167
250
0.3 μV
0 2 4 6 8 10
Time (ms)

Figure 12

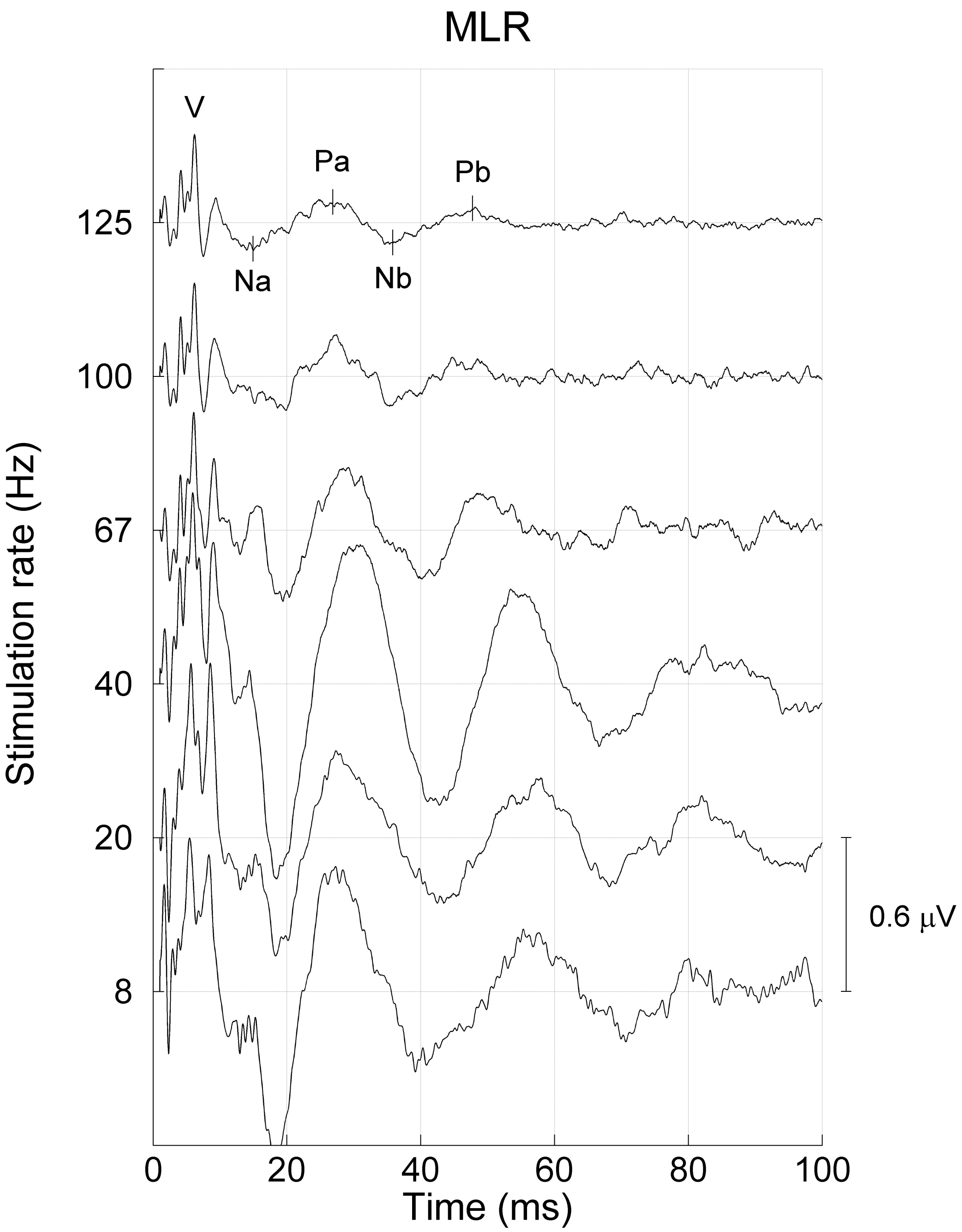
MLR
V
Pa
Pb
Na
Nb
125
100
67
40
20
8
Stimulation rate (Hz)
0
20
40
60
80
100
Time (ms)
0.6 μV